ACS APPLIED POLYMER MATERIALS

pubs.acs.org/acsapm Article

Photocatalytic Nanocomposite Microsponges of Polylactide–Titania for Chemical Remediation in Water

Nirzari Gupta,[‖] Veronika Kozlovskaya,[‖] Maksim Dolmat, Benjamin Yancey, Jonghwa Oh, Claudiu T. Lungu, and Eugenia Kharlampieva*

Cite This: https://dx.doi.org/10.1021/acsapm.0c00937 Read Online

ACCESS | Metrics & More | Article Recommendations | Supporting Information

ABSTRACT: We developed a simple and environmentally friendly approach for synthesis of photocatalytic nanocomposites composed of porous polylactic acid microparticles (PLA) with incorporated anatase titania nanoparticles (TiO_2) for sorption and UV-triggered degradation of organic compounds. Titania is integrated with PLA via 'mixed' and 'grown' methods by mixing anatase and PLA via oil/water emulsion or by growing TiO_2 in a PLA matrix from a titanium precursor under mild reaction conditions. The resulting mixed and grown PLA/TiO_2 microparticles were prepared in the absence or presence of the porogen 2-methylpentane (2MP) and have an average size from 30 to 100 μm. The 'grown titania' is produced as an amorphous–crystalline mixture with ~9% mixed anatase–rutile phase and an average nanoparticle size of ~5 nm. We have demonstrated that the sorption capacity, dye degradability, and composite disintegration can be controlled by varying the microparticle porosity and distribution of incorporated titania nanoparticles. Both types of PLA/TiO_2 composites removed rhodamine 6G from water (up to 60% of the initial amount in six hours of UV exposure time) unlike negligible dye removal observed for titania-free PLA particles. We also found that 'grown' microparticles made with and without 2MP were about 20–30% more efficient in dye removal compared to the corresponding mixed systems. Finally, the presence of titania nanoparticles significantly increased the degradation of PLA. Both 'mixed' and 'grown' microparticles containing 20% TiO_2 exhibited 54 ± 1 and 52 ± 1% weight loss, respectively over 21 days of UV treatment. Owing to their biodegradability and high removal efficiency, these composite microsponges can be applied as nontoxic photocatalytic materials for environmental cleanup of contaminated water. In addition, the synthetic approaches introduced herein offer a simple, scalable, and environmentally friendly method, which might be potentially applied in commercial manufacturing.

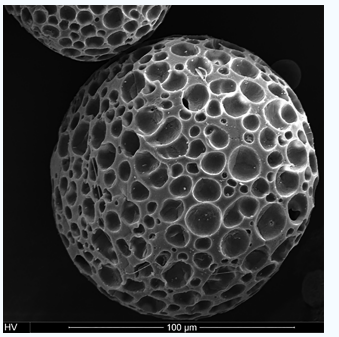

KEYWORDS: *poly(lactic acid), titania, nanocomposites, degradability, porous microparticles*

INTRODUCTION

Increasing the efficiency and scale of water remediation materials remains one of the biggest challenges in the field of water treatment. Although effective, sorbent materials require a costly post-treatment separation and disposal of a contaminated material.[1,2] In this respect, polymer nanocomposites with incorporated photocatalytic titania provide the distinct advantage of eliminating the need for disposal.[3,4] Nanocrystalline titanium oxide is an efficient photocatalyst, which is also nontoxic and stable against photocorrosion and is widely used in food, biomedical applications, and a broad range of consumer products.[5−7] Additionally, a polymer matrix offers a low-cost, mechanically robust, and low-density template to support and suspend the titania, particularly, anatase and rutile, which is responsible for a photocatalytic degradation of organic compounds in the presence of oxygen and solar light.[8−11]

Poly-(D,L-lactic acid) (PLA) is a polyester derived from a renewable source and known for its biocompatibility, tunable degradation, and easily controlled morphology. Although, these characteristics have been widely explored in the biomedical field,[12,13] owing to its low cost, PLA has recently gained attention in environmental applications.[14,15] Integration of titania nanoparticles with PLA matrices promotes enhanced thermal, mechanical, antibacterial, and biodegradation characteristics as well as providing photocatalytic activity.[16,17] In this respect, good dispersion of titania nanoparticles in the PLA matrix is critical to composite performance.[18] However, straightforward methods of inclusion such as direct mixing of hydrophobic PLA with hydrophilic titania nanoparticles often result in phase separation and nanoparticle aggregation, which might adversely affect material performance.[18] Several approaches have been applied to improve the compatibility of these two components, including nanoparticle modification, *in situ* PLA polymerization, and various processing approaches. For example, Hayashi *et al.* modified titania nanoparticles with

Received: August 26, 2020
Accepted: October 19, 2020

propionic acid and *N*-hexylamine to obtain UV-degradable PLA−TiO_2 composite films with well-dispersed titania.[19] Shen *et al.* prepared antibacterial PLA/TiO_2 films by *in situ* polymerization of lactic acid in the presence of TiO_2 nanoparticles coupled with 3-mercaptopropyltrimethoxysilane.[20] Similarly, Shaikh *et al.* found that nanoparticles grafted with PLA through *in situ* polycondensation of lactic acid decolorized the textile dyes methyl orange and methyl green under UV and solar light.[21] In a different approach, Qu *et al.* showed that the dispersion of TiO_2 in melt-blended PLA composites under elongational flow enhanced thermal stability and toughness.[22] Zhu *et al.* also showed that processing methods and distribution of titania inside PLA/TiO_2 melt films were critical parameters for the photocatalytic degradation of methyl orange.[23] Wang and collaborators fabricated photocatalytic PLA−titania films with different concentrations of TiO_2 via the melt-blending method.[24]

One of the promising approaches to efficiently bridge the organic and inorganic components is *in situ* formation of nanocrystalline titania in a polymer matrix.[25] To date, there are numerous methods to form anatase or rutile phase titania, but all of these methods require harsh conditions such as strong acids or bases or high temperatures (>400 °C).[26] These conditions are not compatible with use in polymeric materials as they would cause the polymers to melt, degrade, or polymerize further. In contrast to traditional methods, the *in situ* titania crystallization can be achieved at relatively low temperatures and under mild synthetic conditions. For example, an acid-assisted sol−gel method was used to hydrolyze a titanium alkoxide precursor and convert it into anatase titania at 80 °C for 3 h.[27] Another study reports a room-temperature crystallization of anatase under a solvent-, additive-, and catalyst-free condition that requires 80−90 days.[28] Acid-catalyzed synthesis of TiO_2 crystalline precipitates from titanium alkoxide precursors was demonstrated by Gopal *et al.*[29] and Watson *et al.*[30] at temperatures lower than 100 °C. However, research on *in situ* formation of crystalline titania in PLA matrices remains very limited. In one study, a hydrothermal treatment of electrospun PLA nanofibers with electrosprayed titanium precursor converted the amorphous titania to mixed phase crystalline titania particles with an average size of 0.1−2 μm after heating at 120 °C and under 15 psi pressure.[31] In another study, TiO_2 nanoparticles with sizes ranging from 20 to 200 nm were formed on porous electrospun PLA fibers via hydrolysis of a titanium precursor under ultrasonic irradiation.[32]

Despite the broad collection of studies on PLA−titania composites and growing interest in their synthesis,[33,34] ensuring uniform nanoparticle size and even dispersion in the PLA matrix remains a principle challenge in improving their industrial potential. As a result, the photocatalytic activity of PLA−titania composites has been less studied compared to their mechanical, antibacterial, and degradation properties. In addition, studies on PLA/TiO_2 materials have mostly focused on blends, films, and fibers, whereas microparticles remain underdeveloped due to the challenges mentioned above. Because of this, there remains a significant gain at stake as the spherical morphology of microparticle systems provides larger surface area, simplicity in fabrication, and versatility in composite utilization, which are all essential parameters for water remediation.[7] Therefore, developing a simple, efficient, environmentally friendly, and scalable approach is a critical next step.

In this work, we report on a photocatalytic and environmentally degradable nanocomposite PLA/TiO_2 microparticle with a potential for applications in elimination of hydrophilic pollutants from water. By combining the inherent advantages of a porous PLA matrix with photocatalytic nanocrystalline titania, we explore the nanocomposite's ability toward sorption and UV-triggered degradation of rhodamine 6G dye as well as nanocomposite degradability (Scheme 1). Microsponges are

Scheme 1. Porous PLA Microparticles with Embedded Crystalline TiO_2 Nanoparticles (a) Work as Microsponges for R6G Dye (a Model Water Pollutant) (b). Dye absorbed by the PLA/TiO_2 Microparticle (c) is Degraded Due to Photocatalytic Activity of Crystalline TiO_2 upon UV Treatment (d) Followed by Degradation of PLA Matrix in the Presence of UV Light, Water, and Atmospheric Oxygen (e)

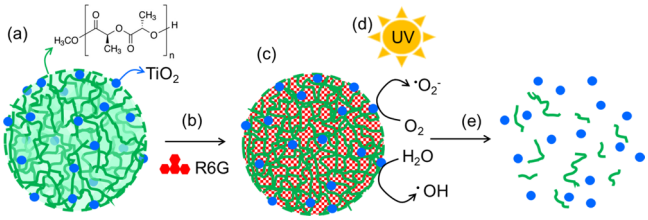

produced by mixing PLA with 13 nm anatase TiO_2 nanoparticles. In an alternative approach, nanotitania is crystallized inside a porous PLA particle from a titanium(IV) tetraisopropoxide (TTIP) precursor under mild synthetic conditions (<60 °C). FTIR spectroscopy, X-ray diffraction analysis, scanning electron microscopy, and confocal laser scanning fluorescence microscopy are used for composite characterization. We study the impact of the synthetic conditions on the size and distribution of TiO_2 nanoparticles as well as on the morphology and functions of the PLA/TiO_2 microparticles. The effects of nanocomposite composition and porosity on chemical and physical properties of the PLA/TiO_2 microparticles are explored with focus on their photocatalytic activity and degradation. The microparticle porosity is controlled by incorporating the phase-change reagent, 2-methylpentane (2MP), which significantly affected microparticle absorption ability. We are motivated by the fact that the material performance for water remediation is highly dependent on the surface area and particle morphologies, which are strongly associated with composite composition and porosity. Owing to their tunable morphology, degradability, and high photocatalytic activity, the PLA/TiO_2 microparticles developed in this work provide a low-cost and potent material for environmental cleanup of contaminated water. In addition, the combination of mild synthesis conditions used in nanocomposite fabrication with the photocatalytic activity of these nanocomposite particles to degrade hydrophilic pollutants from water contributes to environmental sustainability.

EXPERIMENTAL SECTION

Materials. Titanium(IV) oxide anatase powder (TiO_2), titanium(IV) tetraisopropoxide (TTIP), dichloromethane (DCM), and methanol were obtained from Acros Organics. Poly(vinyl alcohol) (PVA) with an average M_w of 25 000 g mol^{-1} was purchased from MP Biomedicals. Rhodamine 6G (R6G) and 2-methylpentane (2MP) were obtained from Millipore-Sigma. The poly-(D,L-lactic acid) (PLA)

https://dx.doi.org/10.1021/acsapm.0c00937
ACS Appl. Polym. Mater. XXXX, XXX, XXX−XXX

with average M_n = 136 000 g mol^{-1} of injection grade was supplied by Jamplast Inc. (Ellisville, USA). Deionized water with a resistivity of 18.2 MΩ·cm (Evoqua) was used for aqueous solution preparation.

Synthesis of PLA/TiO_2 Microparticles. Two methods were used for the synthesis of microparticles using a modified procedure of a previously developed method.[35] The PLA/TiO_2 microparticles obtained using commercial titania nanoparticles were labeled as 'mixed' PLA/TiO_2, while those obtained with TiO_2 nanoparticles grown during the microparticle synthesis were denoted as 'grown' PLA/TiO_2. For the synthesis of mixed microparticles PLA/TiO_2, an emulsification procedure previously developed for PLA particles[36] was modified. Briefly, 0.5 g PLA was dissolved in 17.1 mL DCM, and 0.05 g TiO_2 anatase powder was added into the solution (PLA:TiO_2 = 10:1 weight ratio) followed by vigorous stirring. Next, 0.3665 g 2MP (0.56 mL) was added in predetermined amounts ([PLA + TiO_2]:2MP = 6:4; 8:2; or 10: 0) (40, 20; or 0 wt %) and vortexed for 30 s at 2500 rpm. The mixture was immediately drawn into a 6 mL syringe equipped with a 20G needle and added dropwise to a PVA aqueous solution (300 mL; 0.5% w/v PVA) using a syringe pump (New Era Pump Systems, Inc.) at a rate of 0.3 mL min^{-1} under stirring (600 rpm). After the complete addition, the emulsion was stirred for 12 h to allow total evaporation of the organic solvent followed by filtering (Whatman #4) using vacuum filtration and drying the microparticles overnight on the filter paper without vacuum. TiO_2-free PLA microparticles were prepared as described above using 40% 2MP but without adding TiO_2 anatase powder. The 'grown' PLA/TiO_2 microparticles were synthesized using a two-step procedure. The TTIP solution (0.3788 g; 1 mL DCM) and the PLA solution (0.4273 g; 16.1 mL DCM) were mixed and allowed to form a sol−gel for 30 min in the dark. The 2MP solution was added as described for 'mixed' PLA/TiO_2 microparticles, vortexed for 30 s, transferred into a 6 mL syringe with a 20G needle, and added dropwise to a PVA aqueous solution (300 mL; 0.5% w/v PVA) at the rate of 0.3 mL min^{-1} and stirred at 600 rpm. After stirring for 12 h, the obtained microparticles were collected by filtering and exposed to 150 mL methanol in a capped Erlenmeyer flask for 24 h to induce crystallization of TiO_2. The methanol was removed using rotary evaporation (Buchi Rotavap RII) under vacuum at 50 °C (180 rpm) until the microparticles are completely dry (30 min).

Removal of Rhodamine 6G Dye (R6G) from Water by PLA/TiO_2 Microparticles. To remove R6G dye from water, 10 mg of PLA/TiO_2 microparticles was added to 10 mL of 0.1 mg mL^{-1} R6G aqueous solution followed by the exposure to UV irradiation (λ = 253.5 nm) for 2, 4, or 6 h using a Rayonet RPR 100 photochemical reactor. A particle-free R6G aqueous solution (0.1 mg mL^{-1}) was exposed to the UV light at the same conditions and was used as a control. The 20 mL reaction vials were sealed with rubber caps with an inserted needle and kept in the reactor without stirring. After UV exposure, the samples were centrifuged in the dark at 5000 rpm for 15 min. The supernatant was removed and analyzed by UV−vis spectroscopy (Cary 50) to determine the amount of R6G left in a solution (c_{uv}) using a standard calibration curve. The total amount of R6G removed from R6G aqueous solutions was quantified as the amount of the dye left after subtraction of the amount of dye after UV treatment (c_{uv}) from the initial amount of the dye in the particle-free solution also exposed to the UV light (control).

Degradation of PLA/TiO_2 Microparticles. To study the degradation of the PLA/TiO_2 microsponges, the weighed amounts of the microparticles (~20 mg) dispersed in 7 mL DI water were exposed to UV irradiation (λ = 253.5 nm) using a Rayonet RPR 100 photochemical reactor for 0, 7, 14, 21, and 28 days. The 20 mL reaction vials were sealed with rubber caps with an inserted needle and kept in the reactor without stirring. After that, the weight of the freeze-dried (Labconco) microparticles was measured, and the weight loss catalyzed by the TiO_2 nanofillers was determined as follows: W_d (%) = $(W_i - W_{uv})/W_i \times 100\%$, where W_d is the weight loss due to PLA degradation, W_i is the initial sample weight, and W_{uv} is the sample weight after the UV treatment. The degradation of PLA particles without TiO_2 and TiO_2 anatase powder was studied as controls using the above-mentioned conditions in separate vials.

Characterization of Microparticle Porosity. The surface areas and porosities of PLA/TiO_2 mixed and grown microparticles were analyzed by physisorption using Micromeritics ASAP 2020. Before analysis, the samples were degassed at 30 °C, and nitrogen adsorption was performed at −196 °C. The surface area was determined by the Brunauer−Emmett−Teller (BET) theory, and the total pore volume was calculated at the highest relative pressure. The average pore size was determined by $4V/A$ where V is single point total pore volume (cm^3 g^{-1}) at the highest relative pressure, and A is surface area per unit mass of a sorbent determined by the BET theory (m^2 g^{-1}).

X-Ray Diffraction (XRD). X-ray diffraction spectra of PLA/TiO_2 microparticles were examined using a Panalytical Empyrean Multi-Purpose X-ray Diffractometer with a copper source (λ = 1.54184), BBHD primary optic (Cu β eliminator), and PIXcel 3D linear array detector. The divergence slit of 1/4° with an antiscatter slit of 1° and Soller slits of 0.04° was used on both incident and divergent beam paths. The spectra were measured in terms of 2Θ from 0 to 90° with a 0.01° step-size and a dwell time of 6 s at each step. Phase analysis of the XRD spectra was performed using the HighScore Plus module of the Malvern Panalytical software.

Scanning Electron Microscopy (SEM). The morphology of PLA and PLA/TiO_2 microparticles was examined by a FEI Quanta FEG electron microscope at 10 kV. Before imaging, samples were sputter-coated with 5 nm thin film of silver using a Denton sputter-coater.

Atomic Force Microscopy (AFM). AFM images of TiO_2 nanoparticles were acquired using NT-MDT AFM in tapping mode in air. The NSG30 probe (NT-MDT) with a tip radius less than 5 nm and a nominal spring constant of 22−100 N m^{-1} was used at a scan rate of 1 Hz to analyze TiO_2 nanoparticle size. The TiO_2 anatase nanoparticles were dried on the surfaces of a Si wafer, which was cleaned using a UV Novascan ozone cleaner for 6 h. The size of the TiO_2 nanoparticles was measured using section analysis available in NT-MDT software (IA-P9 version 3.5).

Confocal Laser Scanning Microscopy (CLSM). The distribution of R6G dye within PLA/TiO_2 microparticles in solution was observed using a Nikon A1R multiphoton confocal microscope equipped with 40× oil immersion objective. For that, 2 mg of PLA/TiO_2 microparticles was mixed with 500 μL R6G solution (100 ppm), left for 3 h, and transferred to a multichambered coverglass (Lab-Tek) for imaging.[37]

Fourier Transform Infrared Spectroscopy. FTIR analysis of 'grown' PLA/TiO_2 microparticles, TiO_2 anatase powder, and PLA particles was carried out using a Bruker Alpha ATR-FTIR spectrometer. All samples were air-dried before analysis.

RESULTS AND DISCUSSION

Synthesis of PLA/TiO_2 Mixed Microparticles. To obtain PLA/TiO_2 nanocomposites, we used 'mixed' and 'grown' approaches to introduce TiO_2 nanoparticles into the PLA matrix (Figure 1). In the mixed approach, PLA/TiO_2 microparticles were obtained through oil/water emulsion by mixing crystalline TiO_2 anatase nanoparticles (10 or 20 wt %) with PLA solution in DCM in the absence or presence of 40% porogen, 2MP, followed by adding the organic mixture to an aqueous 0.5 wt % PVA solution under stirring (see details in the Experimental section). In the earlier study, Cho *et al.* found that porosity in golf ball-shaped PLA particles can be controlled by varying the amount of 2MP in the oil/water emulsion.[36]

SEM images of mixed PLA/TiO_2 microparticles are shown in Figure 2. From the SEM analysis, mixed particles have an average size of 100 ± 20 μm. The analysis also reveals that microparticles produced in the presence of 2MP have highly porous morphology with pores equally distributed across the particle surface (Figure 2a,b). In this case, 2MP induced a phase separation in the PLA phase upon evaporation due to its high volatility (boiling point of 62 °C) as was previously

https://dx.doi.org/10.1021/acsapm.0c00937
ACS Appl. Polym. Mater. XXXX, XXX, XXX−XXX

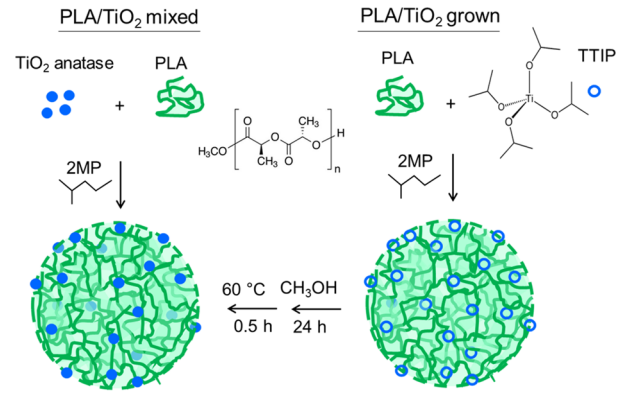

Figure 1. Synthesis of mixed and grown PLA/TiO_2 microparticles. For PLA/TiO_2 mixed microparticles, TiO_2 anatase nanoparticles are directly mixed with PLA in the presence of 2-methylpentane (2MP). For the grown microparticles, PLAs are mixed with the titania precursor, TTIP, in the presence of 2MP resulting in composites with amorphous titania. The amorphous titania is partially converted to crystalline TiO_2 by treatment with methanol for 24 h with a subsequent methanol evaporation at 60 °C.

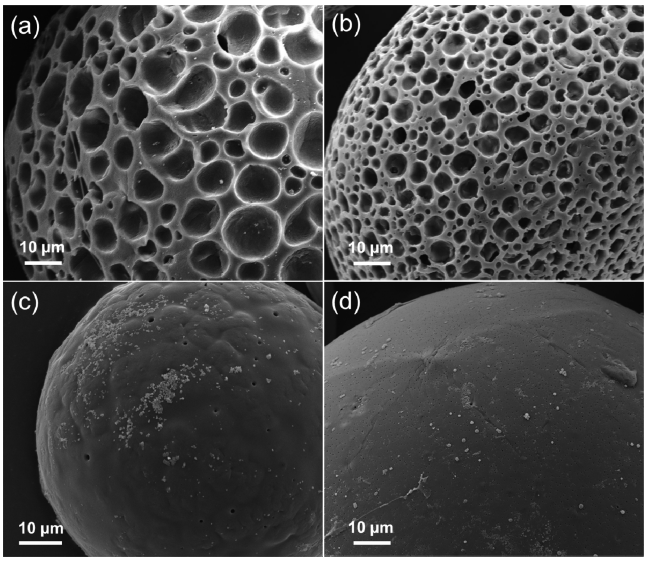

Figure 2. SEM images of (a, b) PLA/TiO_2 mixed microparticles prepared in the presence of 40% 2MP and (c, d) 2MP-free with panels (a, c) 20% and panels (b, d) 10% TiO_2 anatase nanoparticles added.

demonstrated for poly(D,L-lactic-*co*-glycolic acid) (PLGA) microparticles.[36] In contrast, PLA/TiO_2 mixed particles synthesized in the absence of 2MP (2MP-free) are mostly nonporous with relatively smooth surfaces (Figure 2c,d). Porous PLGA particles could be also obtained in a mixture of ethanol and sodium hydroxide.[38] However, unlike 2MP, ethanolic sodium hydroxide may result in de-esterification of PLA and a loss in microparticle integrity.[38]

Although sonication with continuous stirring was used during fabrication of the mixed particles to improve dispersion of TiO_2 anatase nanoparticles throughout the PLA matrix, the surfaces of the particles show some aggregation of titania. The aggregation is more pronounced on the surfaces of nonporous composites (Figure. 2c,d). SEM image analysis showed that for both systems with 10 and 20% titania, the nanoparticle aggregates were up to 1 and up to 10 μm for porous and nonporous systems, respectively. A local aggregation of TiO_2 in organic and inorganic composites was previously reported in poly(ε-caprolactone)(PCL)/TiO_2 particles,[39] carbon/TiO_2,[40] and PLA/TiO_2 blends.[41] Nanoparticle aggregation in polymer composites could be attributed to high interfacial tension between the nonpolar organic phase and the hydrophilic titania nanoparticles when the composites were prepared by mixing.[42] For example, TiO_2-grafted PLA blends showed a nanoscale agglomeration (15−20 nm) of titania on the blend surface when the TiO_2 content was over 10 wt %.[41] The difference between surface energy of PLA and TiO_2 can also reach up to 2 mN m^{-1}, resulting in aggregation.[43] Therefore, the hydrophilicity of TiO_2 anatase nanoparticles mixed in the organic solvent with PLA could lead to the direction of the nanoparticles to PLA surfaces upon DCM evaporation and their aggregation.

Synthesis of PLA/TiO_2 Grown Microparticles with *in Situ* Titania Crystallization. In the 'grown' approach, PLA/TiO_2 composite microparticles were obtained through the oil/water emulsion method, where TiO_2 precursor TTIP was added to a PLA solution in DCM in the presence or absence of 2MP (Figure 1). After the PLA/TiO_2 particles were formed, they were treated with methanol for 24 h at 25 °C followed by methanol evaporation at 60 °C for 0.5 h using a rotavap (Figure 1). SEM images of PLA/TiO_2 grown microparticles are shown in Figure 3.

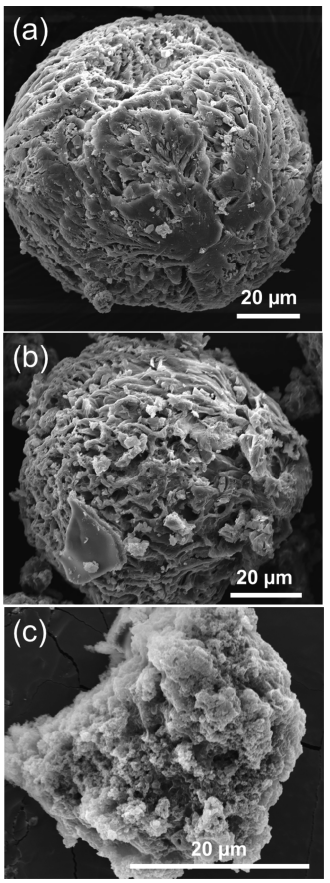

Figure 3. SEM images of PLA/TiO_2-grown microparticles prepared in the absence of (a) 2MP and in the presence of (b) 20 and (c) 40% of 2MP. The microparticles were treated with methanol for 24 h at 25 °C, and methanol was evaporated for 0.5 h at 60 °C.

https://dx.doi.org/10.1021/acsapm.0c00937
ACS Appl. Polym. Mater. XXXX, XXX, XXX−XXX

SEM image analysis shows that the particles prepared in the absence of 2MP have an average size of 100 ± 50 μm and exhibit porous surface morphology (Figure 3a). These 2MP-free 'grown' microparticles have similar size but a much rougher surface compared to their 'mixed' counterparts. The porous morphology and larger surface roughness of the 2MP-free grown particles can be attributed to isopropanol, which is formed as a side product in sol−gel reaction during the formation of amorphous TiO_2 and can act as a porogen-like 2MP. In this reaction, TTIP undergoes hydrolysis in the presence of water and is converted to isopropanol.[44] An increase in the amount of 2MP from 0 to 20 and 40% (Figure 3b,c, respectively) resulted in gradual loss of the spherical shape of the PLA/TiO_2 grown microparticles, which is due to the additional porogenic material participating in the process. The surface of the particles become rougher with increasing amounts of 2MP, which could be beneficial for the particle sorption ability due to the increased surface-to-volume ratio.

In addition, the size of PLA/TiO_2 grown microparticles decreased to the average value of 30 ± 20 μm with the increasing amount of 2MP, which can be attributed to the overall dilution of the organic phase containing PLA and TTIP leading to smaller droplets when emulsified in the water phase[45] and is in agreement with previous reports.[36] The porosity measurements of the PLA/TiO_2 grown and mixed microparticles were carried out by physisorption. BET analysis of porous PLA/TiO_2 mixed and grown microparticles revealed a slightly higher surface area of 27.75 $m^2\ g^{-1}$ for the PLA/TiO_2-grown microparticles prepared in the presence of 40% 2MP and 20% TTIP compared to that of 21.96 $m^2\ g^{-1}$ for the PLA/TiO_2 mixed microparticles (20% 2MP; 20% TiO_2). The average pore sizes were found to be 8.7 and 6.6 nm for the PLA/TiO_2 grown and mixed microparticles, respectively. The pore volume was also larger in the case of the PLA/TiO_2 grown microparticles (0.055 $cm^3\ g^{-1}$) compared to that of the PLA/TiO_2 mixed microparticles (0.030 $cm^3\ g^{-1}$).

Figure 4 demonstrates FTIR analysis of PLA/TiO_2 grown microparticles before and after methanol treatment in comparison to TiO_2 anatase nanoparticles and TiO_2-free porous PLA microparticles. The vibration bands attributed to PLA are observed at 3000, 2970, 1750, 1450, 1200, and 1050 cm^{-1}, while characteristic peaks at 1650, 732, and a broad peak at 509 cm^{-1} represent stretching vibration signals of Ti−O−Ti and Ti−O bonding[46] within both methanol-untreated and methanol-treated particles. A broad signal at 3300 cm^{-1} and a band at 1000 cm^{-1} are attributed to methanol traces in the sample. Although the FTIR analysis confirms the presence of titania, it did not give information about titania crystallinity.

To identify the titania phase, X-ray diffraction (XRD) analysis was applied to the PLA/TiO_2 grown particles before and after methanol treatment. Commercial anatase nanoparticles used for synthesis of PLA/TiO_2 mixed microsponges were used as a control. Figure 5a shows that the XRD pattern of commercial TiO_2 has a sharp peak at 25.2° and peaks at 38 and 48° characteristic of the anatase phase of crystalline TiO_2.[47]

The XRD pattern for PLA/TiO_2 grown microparticles before the methanol treatment (Figure 5b) demonstrates a sharp peak at 16.7° and two peaks at 19.1 and 22.5° characteristic of the common alpha phase of PLA.[48] A low intensity broad peak over a wide range of 2Θ can be attributed to the presence of amorphous TiO_2 and PLA, but no crystalline TiO_2 peaks are seen in this pattern (Figure 5b).

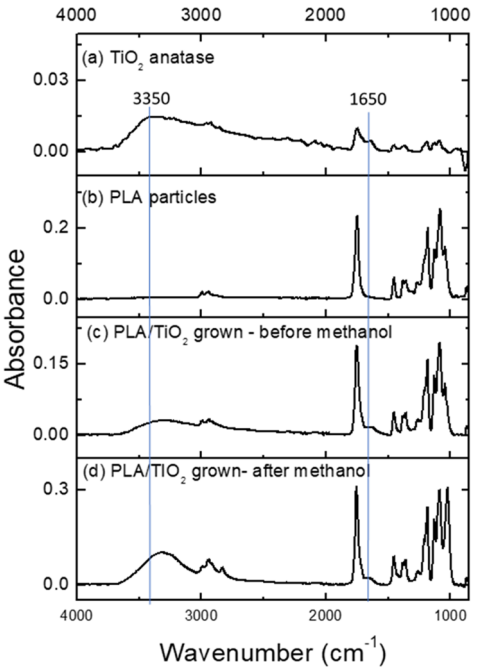

Figure 4. FTIR spectra of (a) TiO_2 anatase, (b) PLA microparticles and PLA/TiO_2 grown microparticles (c) before and (d) after methanol treatment.

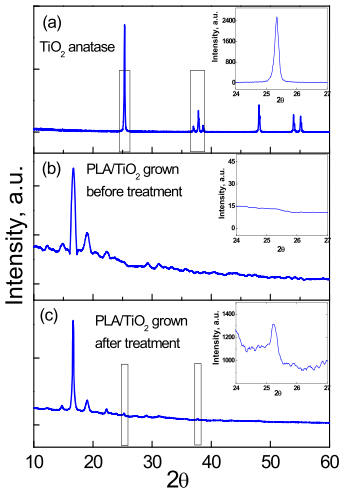

Figure 5. XRD spectra of (a) TiO_2 anatase, (b) PLA/TiO_2 grown microparticles before TiO_2 mineralization in methanol, and (c) PLA/TiO_2 grown microparticles after TiO_2 mineralization in methanol. The inserts demonstrate that the anatase peak at 2Θ = 25.2° appears after TiO_2 mineralization in PLA/TiO_2 grown microparticles.

In contrast, an XRD pattern of the PLA/TiO_2 grown microparticles after methanol treatment clearly shows TiO_2 anatase peaks at 25.2 and 38°, which indicates crystallization of amorphous TiO_2 (Figure 5c). A relative percentage analysis of this XRD pattern demonstrates the presence of 8.6% anatase and 91.4% amorphous (a mixture of PLA and amorphous titania) phases (Figure S1 (Supporting Information). A more detailed TiO_2 phase analysis with HighScore Plus software reveals traces of rutile with characteristic peaks at 27.5 and 36° (Figure S2a).

To determine the total amount of titania, 300 mg of PLA/TiO_2 grown microparticles was heated to 600 °C for 4 h. As a result, ~22% of the initial mass remained (65 mg) and was

https://dx.doi.org/10.1021/acsapm.0c00937
ACS Appl. Polym. Mater. XXXX, XXX, XXX−XXX

attributed to TiO_2 since PLA should be totally decomposed at this temperature.[49] The XRD analysis of the mass remained after the calcination confirmed a complete disintegration of PLA along with the presence of both anatase (75%) and rutile (25%) phases of TiO_2 (Figure S2b), which agrees well with the previous reports on thermal treatment of amorphous titania.[50]

AFM analysis shows that most titania nanoparticles remaining after calcination of the PLA/TiO_2 grown microparticles are 5 ± 1 nm, which is smaller than commercial anatase nanoparticles of 13 ± 3 nm used for the mixed composites. (Figure 6a,b). The AFM image of the calcinated

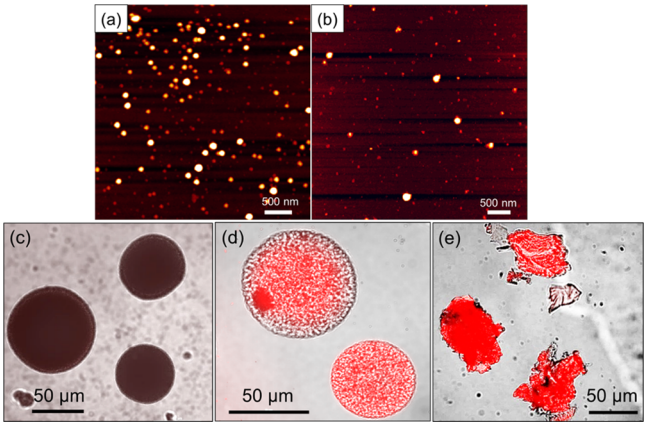

Figure 6. (a,b): AFM topography images of (a) TiO_2 anatase particles used for synthesis of PLA/TiO_2 mixed microsponges and (b) TiO_2 nanoparticles obtained after calcination of PLA/TiO_2 grown microsponges at 600 °C (the z scale is (a) 18 nm and (b) 15 nm). CLSM images of PLA/TiO_2 microparticles after soaking with R6G solution. (c,d): PLA/TiO_2-mixed microparticles prepared (c) in the absence of 2MP and (d) in the presence of 2MP; 40%. (e) PLA/TiO_2 grown microparticles prepared in the presence of 40% 2MP.

particles also shows a small fraction (less than 10%) of larger nanoparticles of 20 ± 4 nm, which might be attributed to some clustering during temperature treatment. This result indicates that the PLA matrices provided an excellent environment for growth and crystallization of 5 nm well-dispersed titania. A critical role of nanoconfinement in crystallization temperatures of inorganic compounds was found previously. For example, ammonium perchlorate salt confined to modified silica nanopores was crystallized from methanol/water solutions due to the adsorption of the salt ions on the nanopore surface.[51] In other studies, a uniformly distributed 5 nm anatase/rutile TiO_2 nanoparticles was spontaneously formed from a titania precursor due to a confinement provided by the protein deposited on polyelectrolyte surfaces.[52,53]

Thus, our results show that amorphous titania dispersed inside the PLA matrix was ∼9% converted into crystalline TiO_2 upon methanol treatment at 60 °C. Titania gels in liquid media were reported to crystallize from amorphous to anatase at temperatures as low as 120 °C.[54] In another study, methanol treatment promoted titania crystallization from a TiBALD precursor in the presence of silaffin proteins.[55] In that study, the presence of primary amine groups acted as binding sites for the negatively charged TiBALD precursor followed by titania formation. In our case, the presence of carboxylic acid end groups of PLA can serve as the sol−gel catalyst during formation of amorphous TiO_2.[56] In addition, good solubility of the TTIP precursor in the DCM organic phase containing PLA provides miscibility of TTIP and PLA. As a result, amorphous TiO_2 can be uniformly distributed throughout the PLA matrix due to condensation of TTIP upon mixing with the aqueous phase.[57] Similarly, in our case, the presence of proton-donating and proton-accepting groups in the confined PLA network could promote titania crystallization from its amorphous phase.

Absorption and Photodegradation of R6G. Considering the photocatalytic potential of titania[58,59] and porous spongelike morphology of the PLA matrix, we explored the ability of PLA/TiO_2 microsponges to remove hydrophilic pollutants such as the fluorescent dye rhodamine 6G from water. For the photocatalytic and self-degradation experiments described below, 'mixed' and 'grown' composites were prepared in the presence of 20% TiO_2 and TTIP, respectively, and in the presence or absence of 40% 2MP.

First, sorption capacity of PLA/TiO_2 mixed and grown composites was analyzed with confocal laser scanning microscopy (CLSM). Both types of particles were soaked in the solution of R6G for 3 h and rinsed with water. Figure 6c demonstrates that 2MP-free mixed particles show no fluorescence signal from R6G, which indicates nonporous morphology. In contrast, the PLA/TiO_2 mixed particles obtained in the presence of 2MP emit red fluorescence throughout the particle volume due to permeation of the dye in the particle interior (Figure 6d), thus demonstrating consistent porous morphology. Similarly, the PLA/TiO_2 grown microsponges successfully absorb the dye and exhibit fluorescence uniformly distributed throughout the particle volume (Figure 6e), implying a highly porous structure.

Next, composite particles prepared in 40% 2MP and 2MP-free particles were mixed with the dye solution (10 mL; 0.1 mg mL^{-1}) and exposed to UV light (253 nm) for 2, 4, and 6 h. We found that the total mass of the removed R6G increased with increasing the UV exposure time from 2 to 6 h for both 'grown' (Figure 7a) and 'mixed' PLA/TiO_2 microparticles prepared in 40% 2MP (Figure 7b). The masses of removed R6G by 'grown' particles from 0.1 mg mL^{-1} R6G initial solution (1 mg of R6G in 10 mL solution) were 0.49 ± 0.01, 0.52 ± 0.02, and 0.60 ± 0.03 mg in 2, 4, and 6 h, respectively (Figure 7a). Similarly, in the case of the corresponding 'mixed' particles, 0.34 ± 0.01, 0.39 ± 0.04, and 0.49 ± 0.06 mg of the dye were removed in 2, 4, and 6 h, respectively (Figure 7b). These data agree with the previous reports on increased photodegradation of various dyes by photocatalytic nanoparticles with the increasing treatment time.[60−63] TiO_2 anatase nanoparticles show a higher dye removal efficiency removing 0.70 ± 0.07, 0.77 ± 0.02, and 0.86 ± 0.01 mg of R6G in 2, 4, 6 hours, respectively. The UV−vis spectra of R6G solutions in the presence of PLA/TiO_2 grown, PLA/TiO_2 mixed, and TiO_2-free PLA microparticles (a) before and (b,c) after UV treatment are shown in Figure S3 (Supporting Information).

After the UV treatment for 6 h, the R6G intensity of all composites decreases, while only negligible changes in the dye intensity are observed for the R6G solution and the dye solution in the presence of titania-free PLA (Figure S3). Both dye absorption and photodegradation should contribute to the total amount of the dye removed from the solutions. A similar trend of increasing R6G removal with the increasing UV exposure time was observed for both 2MP-free microparticles. The total amounts of R6G removed after the 6 h-treatment were 0.52 ± 0.01 and 0.39 ± 0.02 mg for the 'grown' and 'mixed' PLA/TiO_2, respectively (Figure 7). These results suggest that the PLA/TiO_2 grown microparticles prepared in

https://dx.doi.org/10.1021/acsapm.0c00937
ACS Appl. Polym. Mater. XXXX, XXX, XXX−XXX

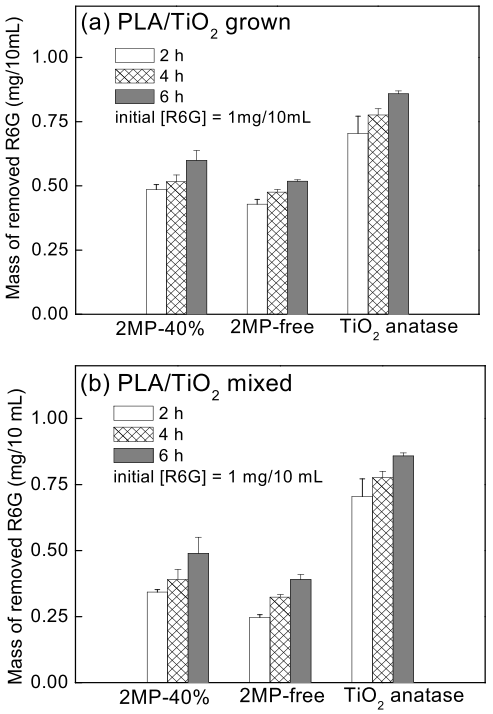

Figure 7. Total removal of R6G from aqueous solution (0.1 mg/mL) by (a) PLA/TiO_2 grown and (b) PLA/TiO_2 mixed microparticles after 2, 4, and 6 h of exposure to UV light (253 nm). Removal of R6G by 40% 2MP and 2MP-free particles were compared with that of commercial anatase.

the absence of the porogen were ~25% more effective in removal of the dye compared to the 2MP-free mixed particles. This result can be explained by the fact that 2MP-free grown particles have high porosity due to isopropanol release during particle synthesis (Figure 3a) unlike very limited porosity observed in the 2MP-free mixed particles (Figures 24c,d and a).

Figure 7 also shows that 40% 2MP-composites remove the dye about 20% more efficiently than their 2MP-free counterparts. The amounts of R6G removed after the 6 h-treatment decreased from 0.60 ± 0.01 to 0.52 ± 0.01 mg and from 0.49 ± 0.06 to 0.39 ± 0.02 mg for the 'grown' and 'mixed' PLA/TiO_2, respectively (Figure 7). Previous studies also pointed to the importance of PLA porous morphology on the efficacy of dye degradation. The TiO_2-loaded porous PLA fibers showed a successful photocatalytic activity by degrading methylene blue dye.[32] In contrast, enzymatic PLA erosion was required for PLA–titania films to achieve photodegradation of that dye.[24]

Thus, our data indicate that dye removal efficiency by the 'grown' composites made with and without 2MP is consistently higher for all exposure times (about 20–30%) than that observed by the corresponding 'mixed' systems. There can be two reasons for this result. First, the inherent porosity of the PLA/TiO_2 grown microsponges due to isopropanol release as mentioned above (Figure 3a) can contribute to this result unlike the smooth surfaces of the 2MP-free PLA/TiO_2 mixed microparticles (Figure 2c,d). Conversely, clustering of TiO_2 anatase on the surfaces of 2MP-free PLA/TiO_2 mixed microparticles could lead to decreased efficiency as photocatalysts. For instance, carbon nanotubes/TiO_2 composites were reported to exhibit a twofold greater R6G absorption and degradation in response to reduced aggregation and improved crystallinity of TiO_2 nanoparticles.[64−66] We also found from the AFM analysis described above that TiO_2 nanoparticles used in PLA/TiO_2 mixed composites have ~3 times larger size compared to the nanoparticles produced *in situ* within PLA/TiO_2 grown matrices (Figure 6a,b). Thus, the use of the titanium precursor provides a stronger attachment of the formed nanoparticles to the PLA template, which enhances interfacial strength and improves the integration of the components. In addition, the presence of anatase and rutile TiO_2 in the PLA/TiO_2 grown microsponges after the methanol treatment could contribute to the removal of R6G. A mixed anatase–rutile phase of commercial TiO_2 nanoparticles was previously shown to be more photocatalytically active compared to anatase alone.[67]

Degradation of PLA/TiO_2 Microparticles. Finally, to account for the degradable nature of PLA and catalytic activity of titania, we explored the capability of UV-treated PLA/TiO_2 composites toward degradation. In the previous studies, titania nanoparticles have been shown to accelerate decomposition of biodegradable polymer matrices under UV irradiation. For example, poly(butyl succinate)/TiO_2 composites containing 5% titania degraded 67% more than the pure polymer after 26 days of UV light.[68] In our study, the degradation of PLA/TiO_2 microsponges (20 mg) was analyzed in comparison to TiO_2 anatase nanoparticles and TiO_2-free PLA particles after particles dispersed in DI water were exposed to UV light (λ = 253.5 nm) for 7, 14, and 21 days in the presence of atmospheric oxygen. The weight of the freeze-dried microparticles was measured, and the weight loss after UV irradiation catalyzed by the TiO_2 nanofillers was determined.

Figure 8 shows that both the PLA/TiO_2 mixed and PLA/TiO_2 grown microsponges are gradually losing their weight

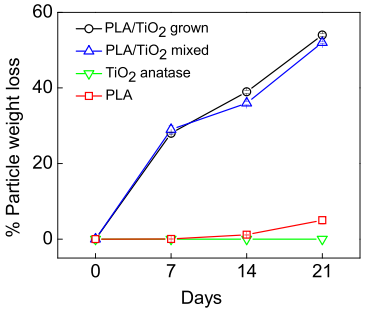

Figure 8. Degradation of PLA/TiO_2 microparticles (20 mg) under UV light (253 nm) in water (8 mL). TiO_2 anatase nanoparticles and TiO_2-free porous PLA microparticles (PLA) were used as controls. All particles were prepared in the presence of 40% 2MP. PLA/TiO_2 mixed contains 20% titania, and the PLA/TiO_2 grown were made in the presence of 20% TTIP.

over 21 days of the treatment. The PLA/TiO_2 grown microsponges lost 28 ± 1, 39 ± 4, and 54 ± 1% weight in 7, 14, and 21 days, respectively. The PLA/TiO_2 mixed particles were degrading in a similar fashion with weight losses of 29 ± 1, 36 ± 1, and 52 ± 1% of mass during 7, 14, and 21 days of the treatment, respectively. There was no mass loss from TiO_2 anatase nanoparticles used as control, and only 5 ± 1% weight loss in 21 days was observed for TiO_2-free PLA microparticles under these conditions.

Our data indicate that the degradation of both nanocomposites is mainly initiated by the TiO_2 photocatalyst and that the mass loss increases with UV exposure time. Our

https://dx.doi.org/10.1021/acsapm.0c00937
ACS Appl. Polym. Mater. XXXX, XXX, XXX−XXX

findings correlate well with the previous photocatalytic studies on PLA−titania nanocomposites. Guo *et al.* showed that the weight loss of PLA/TiO_2 blends with 2 wt % of TiO_2 was linear with increase in irradiation time and reached 17% in 80 days as opposed to no significant changes in weight observed for pure PLA under these conditions.[69] The photodegradability of the composites was attributed to the accelerated effect of well-dispersed titania leading to covalent bond scission in the PLA matrix and formation of volatile products.[69]

Our results also show that both systems efficiently degrade at the same rate, which suggests that in both methods, titania is dispersed well enough to expedite the degradation. The heterogeneity and the size of titania nanofillers were shown to affect the degradation rate of polymer matrices.[24] Well-dispersed nanoparticles of small size typically increase the photocatalytic degradation of composites while nanoparticle clustering slows it down due to the decreased surface area. For example, the photocatalytic degradation of PLA/TiO_2 composites containing well-dispersed 2 wt % nanoparticles was faster compared to the composites with 8 wt % titania, which showed titania agglomerates.[69] Similarly, photocatalytic degradation of melt-blended PBS−titania nanocomposites was increased by improving the dispersibility by accelerating the rotation as well as decreasing the size of titania nanoparticles to 5 nm.[68] In our study, both 'mixed' and 'grown' composites are 55% photodegraded in 21 days unlike 5% weight loss for a pure PLA, which indicates a considerable accelerating effect of titania on the decomposition. A small size of TiO_2 anatase−rutile nanoparticles (<5 nm) along with their homogeneous distribution in the porous PLA matrix could be responsible for an accelerated hydrolysis and thus high degradation performance of both PLA/TiO_2 systems.

CONCLUSIONS

By using mild synthesis conditions, we developed photocatalytic and degradable PLA/titania microparticles for sorption and remediation of organic compounds from water. Crystalline TiO_2 was integrated into porous PLA matrices using two approaches, both in the presence or absence of 2MP as a porogen: (1) by mixing TiO_2 anatase nanoparticles with PLA to obtain PLA/TiO_2 mixed microsponges and (2) by *in situ* crystallization of titania nanoparticles from the TTIP precursor inside porous PLA under methanol treatment at 60 °C. In the latter case, titania was produced as an amorphous−crystalline mixture with ∼9% mixed anatase−rutile phase, and an average nanoparticle size of ∼5 nm as determined by AFM and XRD. The 2MP-free 'grown' particles have a similar size of 100 μm but a much rougher surface compared to their 'mixed' counterparts. PLA/TiO_2 mixed particles prepared in the presence of 40% 2MP had highly porous morphology unlike nonporous 2MP-free 'mixed' microparticles. In contrast, both 'grown' composites prepared in the presence and absence of 2MP exhibited porous morphology due to isopropanol release during particle formation. An increase in the amount of 2MP from 0 to 20 and 40% resulted in the gradual loss of the spherical shape of the PLA/TiO_2 grown microparticles and in a size decrease to 30 μm. Both types of PLA/TiO_2 composites efficiently absorbed and photodegraded rhodamine 6G from water (in a range from 35 to 60% of the initial dye amount) unlike negligible dye removal observed for titania-free PLA particles. The total mass of the removed dye increased with increasing the UV exposure time from 2 to 6 h with 20% more efficient dye removal by 40% 2MP-composites compared to their 2MP-free counterparts. We also found that 'grown' particles made with and without 2MP were about 20−30% more efficient in total dye removal for all exposure times compared to the corresponding 'mixed' systems. Finally, the nanofillers were found to increase the degradation of biodegradable PLA polymer matrix compared to the TiO_2-free porous PLA microsponges. Both composites containing 20% TiO_2 gradually degraded over 21 days of the UV treatment with 54 ± 1 and 52 ± 1% weight loss for the 'grown' and 'mixed' systems, respectively. Owing to their biodegradability and high removal efficiency, these composite microsponges have high potential for applications as nontoxic photocatalytic materials for the cleanup of contaminated public wastewater from pharmaceuticals and fertilizers. We believe that the material's ability to absorb and degrade contaminants, followed by self-degradation is an important property of the material that can potentially eliminate the additional step of material retrieval after it was applied, which could save on resources and the cost of retrieval. In addition, synthetic approaches introduced herein offer a simple, environmentally friendly, and scalable method, which could be easily adopted for future manufacturing.

ASSOCIATED CONTENT

Supporting Information

The Supporting Information is available free of charge at https://pubs.acs.org/doi/10.1021/acsapm.0c00937.

Information about XRD phase analysis of the composite microparticles, UV−vis spectra of R6G supernatants after UV-treated composite microparticles, R6G calibration curve, mass of dye removed by titania-free PLA after UV exposure, and optical images of PLA−TiO2 grown and mixed microparticles before and after calcination (PDF)

AUTHOR INFORMATION

Corresponding Author

Eugenia Kharlampieva − *Department of Chemistry and Center for Nanoscale Materials and Biointegration, University of Alabama at Birmingham, Birmingham, Alabama 35294, United States;* orcid.org/0000-0003-0227-0920; Email: ekharlam@uab.edu

Authors

Nirzari Gupta − *Department of Chemistry, University of Alabama at Birmingham, Birmingham, Alabama 35294, United States*

Veronika Kozlovskaya − *Department of Chemistry, University of Alabama at Birmingham, Birmingham, Alabama 35294, United States;* orcid.org/0000-0001-9089-4842

Maksim Dolmat − *Department of Chemistry, University of Alabama at Birmingham, Birmingham, Alabama 35294, United States*

Benjamin Yancey − *Department of Chemistry, University of Alabama at Birmingham, Birmingham, Alabama 35294, United States*

Jonghwa Oh − *Department of Environmental Health Sciences, University of Alabama at Birmingham, Birmingham, Alabama 35294, United States*

Claudiu T. Lungu − *Department of Environmental Health Sciences, University of Alabama at Birmingham, Birmingham, Alabama 35294, United States*

https://dx.doi.org/10.1021/acsapm.0c00937
ACS Appl. Polym. Mater. XXXX, XXX, XXX−XXX

Complete contact information is available at:
https://pubs.acs.org/10.1021/acsapm.0c00937

Author Contributions

[‖]N.G. and V.K. equally contributed to this work.

Notes

The authors declare the following competing financial interest(s): N.G., V.K., M.D., J.O., and C.L. declare no conflict of interest. E.K. and B.Y. filed intellectual property US patent in June 18, 2012 (Appl. no.: 14/125,371. Pub. no.: US 2014/0102991 A1) for the procedure development that was identified in this study; however, there is no conflict of financial interest.

■ ACKNOWLEDGMENTS

The work was supported by NSF OIA award #1632825 and NSF DMR award #1828232. We also acknowledge UAB Scanning Electron Microscopy and UAB High-Resolution Imaging Facility.

■ REFERENCES

(1) Roosen, J.; Spooren, J.; Binnemans, K. Adsorption performance of functionalized chitosan−silica hybrid materials toward rare earths. *J. Mater. Chem. A* **2014**, *2*, 19415−19426.
(2) Sirés, I.; Brillas, E. Remediation of water pollution caused by pharmaceutical residues based on electrochemical separation and degradation technologies: a review. *Environ. Int.* **2012**, *40*, 212−229.
(3) Abdal-hay, A.; Makhlouf, A. S. H.; Khalil, K. A. Novel, Facile, Single-Step Technique of Polymer/TiO_2 Nanofiber Composites Membrane for Photodegradation of Methylene Blue. *ACS Appl. Mater. Interfaces* **2015**, *7*, 13329−13341.
(4) Singh, S.; Mahalingam, H.; Singh, P. K. Polymer-supported titanium dioxide photocatalysts for environmental remediation: A review. *Appl. Catal. A Gen.* **2013**, *462-463*, 178−195.
(5) Wu, S.; Weng, Z.; Liu, X.; Yeung, K. W. K.; Chu, P. K. Functionalized TiO_2 based nanomaterials for biomedical applications. *Adv. Funct. Mater.* **2014**, *24*, 5464−5481.
(6) Kale, B. M.; Wiener, J.; Militky, J.; Rwawiire, S.; Mishra, R.; Jacob, K. I.; Wang, Y. Coating of cellulose-TiO_2 nanoparticles on cotton fabric for durable photocatalytic self-cleaning and stiffness. *Carbohydr. Polym.* **2016**, *150*, 107−113.
(7) Vats, T.; Sharma, S. N.; Kumar, M.; Kar, M.; Jain, K.; Singh, V. N.; Mehta, B. R.; Narula, A. K. Comparison of photostability, optical and structural properties of TiO_2/conjugated polymer hybrid composites prepared via different methods. *Thin Solid Films* **2010**, *519*, 1100−1105.
(8) Nosaka, Y.; Nosaka, A. Understanding hydroxyl radical (• OH) generation processes in photocatalysis. *ACS Energy Lett.* **2016**, *1*, 356−359.
(9) O'Regan, B.; Grätzel, M. A low-cost, high-efficiency solar cell based on dye-sensitized colloidal TiO_2. *Nature* **1991**, *353*, 737−740.
(10) Goto, H.; Hanada, Y.; Ohno, T.; Matsumura, M. Quantitative analysis of superoxide ion and hydrogen peroxide produced from molecular oxygen on photoirradiated TiO_2 particles. *J. Catal.* **2004**, *225*, 223−229.
(11) Rephaeli, E.; Fan, S. Tungsten black absorber for solar light with wide angular operation range. *Appl. Phys. Lett.* **2008**, *92*, 211107.
(12) Orozco, V. H.; Kozlovskaya, V.; Kharlampieva, E.; López, B. L.; Tsukruk, V. V. Biodegradable self-reporting nanocomposite films of poly(lactic acid) nanoparticles engineered by layer-by-layer assembly. *Polymer* **2010**, *51*, 4127−4139.
(13) Wang, Y.; Shi, X.; Ren, L.; Yao, Y.; Zhang, F.; Wang, D. A. Poly (lactide-co-glycolide)/titania composite microsphere-sintered scaffolds for bone tissue engineering applications. *J. Biomed. Mater. Res., Part B* **2010**, *9999B*, 84−92.
(14) Gu, J.; Xiao, P.; Chen, P.; Zhang, L.; Wang, H.; Dai, L.; Song, L.; Huang, Y.; Zhang, J.; Chen, T. Functionalization of Biodegradable PLA Nonwoven Fabric as Superoleophilic and Superhydrophobic Material for Efficient Oil Absorption and Oil/Water Separation. *ACS Appl. Mater. Interfaces* **2017**, *9*, 5968−5973.
(15) Zhu, C.; Jiang, W.; Hu, J.; Sun, P.; Li, A.; Zhang, Q. Polylactic Acid Nonwoven Fabric Surface Modified with Stereocomplex Crystals for Recyclable Use in Oil/Water Separation. *ACS Appl. Poly. Mat.* **2020**, *2*, 2509.
(16) Fonseca, C.; Ochoa, A.; Ulloa, M. T.; Alvarez, E.; Canales, D.; Zapata, P. A. Poly (lactic acid)/TiO_2 nanocomposites as alternative biocidal and antifungal materials. *Mater. Sci. Eng. C.* **2015**, *57*, 314−320.
(17) Foruzanmehr, M.; Vuillaume, P. Y.; Elkoun, S.; Robert, M. Physical and mechanical properties of PLA composites reinforced by TiO_2 grafted flax fibers. *Mater. Des.* **2016**, *106*, 295−304.
(18) Kaseem, M.; Hamad, K.; Ur Rehman, Z. Review of Recent Advances in Polylactic Acid/TiO_2 Composites. *Materials* **2019**, *12*, 3659.
(19) Nakayama, N.; Hayashi, T. Preparation and characterization of poly (L-lactic acid)/TiO_2 nanoparticle nanocomposite films with high transparency and efficient photodegradability. *Polym. Degrad. Stab.* **2007**, *92*, 1255−1264.
(20) Zhuang, W.; Liu, J.; Zhang, J. H.; Hu, B. X.; Shen, J. Preparation, characterization, and properties of TiO_2/PLA nanocomposites by in situ polymerization. *Polym. Compos.* **2009**, *30*, 1074−1080.
(21) Shaikh, T.; Rathore, A.; Kaur, H. Poly (lactic acid) grafting of TiO_2 nanoparticles: A shift in dye degradation performance of TiO_2 from UV to solar light. *ChemistrySelect* **2017**, *2*, 6901−6908.
(22) Zhang, H.; Huang, J.; Yang, L.; Chen, R.; Zou, W.; Lin, X.; Qu, J. Preparation, characterization and properties of PLA/TiO_2 nanocomposites based on a novel vane extruder. *RSC Adv.* **2015**, *5*, 4639−4647.
(23) Zhu, Y.; Buonocore, G. G.; Lavorgna, M.; Ambrosio, L. Poly(lactic acid)/titanium dioxide nanocomposite films: Influence of processing procedure on dispersion of titanium dioxide and photocatalytic activity. *Polym. Compos.* **2011**, *32*, 519−528.
(24) Zhang, C.; Cai, X.; Wang, F. Preparation and evaluation of the self-cleaning poly (lactic acid)(PLA) film blended with Titanium dioxide nano particles. *Ind. Text.* **2016**, *67*, 121−126.
(25) Ghosal, A.; Ahmad, S. High performance anti-corrosive epoxy-titania hybrid nanocomposite coatings. *New J. Chem.* **2017**, *41*, 4599−4610.
(26) Ismagilov, Z. R.; Tsikoza, L. T.; Shikina, N. V.; Zarytova, V. F.; Zinoviev, V. V.; Zagrebelnyi, S. N. Synthesis and stabilization of nanosized titanium dioxide. *Russ. Chem. Rev.* **2009**, *78*, 873−885.
(27) Leyva-Porras, C.; Toxqui-Teran, A.; Vega-Becerra, O.; Miki-Yoshida, M.; Rojas-Villalobos, M.; García-Guaderrama, M.; Aguilar-Martínez, J. A. Low-temperature synthesis and characterization of anatase TiO_2 nanoparticles by an acid assisted sol-gel method. *J. Alloys Compd.* **2015**, *647*, 627−636.
(28) Su, J.; Zou, X.; Li, G.-D.; Jiang, Y.-M.; Cao, Y.; Zhao, J.; Chen, J.-S. Room-temperature spontaneous crystallization of porous amorphous titania into a high-surface-area anatase photocatalyst. *Chem. Commun.* **2013**, *49*, 8217−8219.
(29) Gopal, M.; Chan, W. J. B.; de Jonghe, L. C. Room temperature synthesis of crystalline metal oxides. *J. Mater. Sci.* **1997**, *32*, 6001−6008.
(30) Watson, S. S.; Beydoun, D.; Scott, J. A.; Amal, R. The effect of preparation method on the photoactivity of crystalline titanium dioxide particles. *Chem. Eng.* **2003**, *95*, 213−220.
(31) Gupta, K. K.; Mishra, P. K.; Srivastava, P.; Gangwar, M.; Nath, G.; Maiti, P. Hydrothermal in situ preparation of TiO2 particles onto poly(lactic acid) electrospun nanofibres. *Appl. Surf. Sci.* **2013**, *264*, 375−382.
(32) Hou, X.; Cai, Y.; Mushtaq, M.; Song, X.; Yang, Q.; Huang, F.; Wei, Q. Deposition of TiO_2 nanoparticles on porous polylactic acid fibrous substrates and its photocatalytic capability. *J. Nanosci. Nanotechnol.* **2018**, *18*, 5617−5623.

(33) Fiorenza, R.; Di Mauro, A.; Cantarella, M.; Privitera, V.; Impellizzeri, G. Selective photodegradation of 2,4-D pesticide from water by molecularly imprinted TiO_2. *J. Photochem. Photobiol. A* **2019**, *380*, 111872.
(34) El-Mekkawi, D. M.; Abdelwahab, N. A.; Mohamed, W. A. A.; Taha, N. A.; Abdel-Mottaleb, M. S. A. Solar photocatalytic treatment of industrial wastewater utilizing recycled polymeric disposals as TiO_2 supports. *J. Cleaner Prod.* **2020**, *249*, 119430.
(35) Kharlampieva, E.; Yancey, B. Biodegradable photocatalytic nanocomposite microsponges of polyactic acid. U.S. Patent US20140102991A1, April 17, 2014.
(36) Kim, M. R.; Lee, S.; Park, J.-K.; Cho, K. Y. Golf ball-shaped PLGA microparticles with internal pores fabricated by simple O/W emulsion. *Chem. Commun.* **2010**, *46*, 7433−7435.
(37) Gupta, N.; Kozlovskaya, V.; Dolmat, M.; Kharlampieva, E. Shape Recovery of Spherical Hydrogen-Bonded Multilayer Capsules after Osmotically Induced Deformation. *Langmuir* **2019**, *35*, 10910−10919.
(38) Tham, C. Y.; Hamid, Z. A. A.; Ahmad, Z. A.; Ismail, H. Surface Engineered Poly(lactic acid) (PLA) Microspheres by Chemical Treatment for Drug Delivery System. *Key Eng. Mater.* **2014**, *594-595*, 214−218.
(39) Meng, B.; Tao, J.; Deng, J.; Wu, Z.; Yang, M. Toughening of polylactide with higher loading of nano-titania particles coated by poly(ε-caprolactone). *Mater. Lett.* **2011**, *65*, 729−732.
(40) An, G.; Ma, W.; Sun, Z.; Liu, Z.; Han, B.; Miao, S.; Miao, Z.; Ding, K. Preparation of titania/carbon nanotube composites using supercritical ethanol and their photocatalytic activity for phenol degradation under visible light irradiation. *Carbon* **2007**, *45*, 1795−1801.
(41) Liao, H. T.; Wu, C. S. New biodegradable blends prepared from polylactide, titanium tetraisopropylate, and starch. *J. Appl. Polym. Sci.* **2008**, *108*, 2280−2289.
(42) Bhattacharya, M. Polymer Nanocomposites-A Comparison between Carbon Nanotubes, Graphene, and Clay as Nanofillers. *Materials* **2016**, *9*, 262.
(43) Mofokeng, J. P.; Luyt, A. S. Morphology and thermal degradation studies of melt-mixed poly(lactic acid)(PLA)/poly(ε-caprolactone)(PCL) biodegradable polymer blend nanocomposites with TiO_2 as filler. *Polym. Test.* **2015**, *45*, 93−100.
(44) Chaudhari, P.; Chaudhari, V.; Mishra, S. Low Temperature Synthesis of Mixed Phase Titania Nanoparticles with High Yield, its Mechanism and Enhanced Photoactivity. *Mater. Res.* **2016**, *19*, 446−450.
(45) Rosca, I. D.; Watari, F.; Uo, M. Microparticle formation and its mechanism in single and double emulsion solvent evaporation. *J. Controlled Release* **2004**, *99*, 271−280.
(46) Meaurio, E.; López-Rodríguez, N.; Sarasua, J. R. Infrared Spectrum of Poly(l-lactide): Application to Crystallinity Studies. *Macromolecules* **2006**, *39*, 9291−9301.
(47) Yan, W.; Petkov, V.; Mahurin, S. M.; Overbury, S. H.; Dai, S. Powder XRD analysis and catalysis characterization of ultra-small gold nanoparticles deposited on titania-modified SBA-15. *Catal. Commun.* **2005**, *6*, 404−408.
(48) Wasanasuk, K.; Tashiro, K.; Hanesaka, M.; Ohhara, T.; Kurihara, K.; Kuroki, R.; Tamada, T.; Ozeki, T.; Kanamoto, T. Crystal structure analysis of poly(L-lactic acid) form on the basis of the 2-dimensional wide-angle synchrotron X-ray and neutron diffraction measurements. *Macromolecules* **2011**, *44*, 6441−6452.
(49) Yan, Y.; Gu, X.; Li, L.; Li, H.; Sun, J.; Zhang, S. Preparation and characterization of intumescent flame retardant biodegradable poly (lactic acid) nanocomposites based on sulfamic acid intercalated layered double hydroxides. *Fibers Polym.* **2017**, *18*, 2060−2069.
(50) Ovenstone, J.; Yanagisawa, K. Effect of hydrothermal treatment of amorphous titania on the phase change from anatase to rutile during calcination. *Chem. Mater.* **1999**, *11*, 2770−2774.
(51) Stanford, V. L.; Vyazovkin, S. Crystallization of ammonium perchlorate from solution confined to native and organically modified silica nanopores. *Thermochim. Acta* **2019**, *677*, 109−116.
(52) Kharlampieva, E.; Slocik, J. M.; Singamaneni, S.; Poulsen, N.; Kröger, N.; Naik, R. R.; Tsukruk, V. V. Protein-Enabled Synthesis of Monodisperse Titania Nanoparticles On and Within Polyelectrolyte Matrices. *Adv. Funct. Mater.* **2009**, *19*, 2303−2311.
(53) Kharlampieva, E.; Jung, C. M.; Kozlovskaya, V.; Tsukruk, V. V. Secondary structure of silaffin at interfaces and titania formation. *J. Mater. Chem.* **2010**, *20*, 5242−5250.
(54) Yin, S.; Inoue, Y.; Uchida, S.; Fujishiro, Y.; Sato, T. Crystallization of titania in liquid media and photochemical properties of crystallized titania. *J. Mater. Res.* **1998**, *13*, 844−847.
(55) Kröger, N.; Dickerson, M. B.; Ahmad, G.; Cai, Y.; Haluska, M. S.; Sandhage, K. H.; Poulsen, N.; Sheppard, V. C. Bioenabled synthesis of rutile (TiO_2) at ambient temperature and neutral pH. *Angew. Chem., Int. Ed.* **2006**, *45*, 7239−7243.
(56) Cui, Y.; Liu, L.; Li, B.; Zhou, X.; Xu, N. Fabrication of tunable core-shell structured TiO_2 mesoporous microspheres using linear polymer polyethylene glycol as templates. *J. Phys. Chem. C* **2010**, *114*, 2434−2439.
(57) Mahshid, S.; Askari, M.; Ghamsari, M. S. Synthesis of TiO_2 nanoparticles by hydrolysis and peptization of titanium isopropoxide solution. *J. Mater. Process. Technol.* **2007**, *189*, 296−300.
(58) Vogel, R.; Meredith, P.; Harvey, M. D.; Rubinsztein-Dunlop, H. Absorption and fluorescence spectroscopy of rhodamine 6G in titanium dioxide nanocomposites. *Spectrochim. Acta A* **2004**, *60*, 245−249.
(59) Khan, S. A.; Ali, S.; Sohail, M.; Morsy, M. A.; Yamani, Z. H. Fabrication of TiO_2/Ag/Ag_2O nanoparticles to enhance the photocatalytic activity of Degussa P25 titania. *Aust. J. Chem.* **2016**, *69*, 41−46.
(60) Chiu, Y.-H.; Chang, T.-F. M.; Chen, C.-Y.; Sone, M.; Hsu, Y.-J. Mechanistic insights into photodegradation of organic dyes using heterostructure photocatalysts. *Catalysts* **2019**, *9*, 430.
(61) Kumar, A.; Pandey, G. A review on the factors affecting the photocatalytic degradation of hazardous materials. *Mater. Sci. Eng. Int. J.* **2017**, *1*, 106−114.
(62) Vanamudan, A.; Pamidimukkala, P. Chitosan, nanoclay and chitosan−nanoclay composite as adsorbents for Rhodamine-6G and the resulting optical properties. *Int. J. Biol. Macromol.* **2015**, *74*, 127−135.
(63) Khalfaoui-Boutoumi, N.; Boutoumi, H.; Khalaf, H.; David, B. Synthesis and characterization of TiO_2-Montmorillonite/Polythiophene-SDS nanocomposites: Application in the sonophotocatalytic degradation of rhodamine 6G. *Appl. Clay Sci.* **2013**, *80-81*, 56−62.
(64) Guo, M. Y.; Liu, F.; Leung, Y. H.; Ng, A. M. C.; Djurišić, A. B.; Chan, W. K. TiO_2-carbon nanotube composites for visible photocatalysts - Influence of TiO_2 crystal structure. *Curr. Appl. Phys.* **2013**, *13*, 1280−1287.
(65) Wu, Y.; Abraham, D.; Carta, G. Particle size effects on protein and virus-like particle adsorption on perfusion chromatography media. *J. Chromatogr. A* **2015**, *1375*, 92−100.
(66) Ye, G.; Duan, X.; Zhu, K.; Zhou, X.; Coppens, M.-O.; Yuan, W. Optimizing spatial pore-size and porosity distributions of adsorbents for enhanced adsorption and desorption performance. *Chem. Eng. Sci.* **2015**, *132*, 108−117.
(67) Siah, W. R.; Lintang, H. O.; Shamsuddin, M.; Yuliati, L. High photocatalytic activity of mixed anatase-rutile phases on commercial TiO_2 nanoparticles. *IOP Conf. Ser.: Mater. Sci. Eng.* **2016**, *107*, 012005.
(68) Miyauchi, M.; Li, Y.; Shimizu, H. Enhanced Degradation in Nanocomposites of TiO_2 and Biodegradable Polymer. *Environ. Sci. Technol.* **2008**, *42*, 4551−4554.
(69) Luo, Y.; Cao, Y.; Guo, G. Effects of TiO_2 nanoparticles on the photodegradation of poly(lactic acid). *J. Appl. Polym. Sci.* **2018**, *135*, 46509.

https://dx.doi.org/10.1021/acsapm.0c00937
ACS Appl. Polym. Mater. XXXX, XXX, XXX−XXX